



Aalborg Universitet

AALBORG UNIVERSITY  
DENMARK

## Automated rainfall simulator for variable rainfall on urban green areas

Nielsen, Kristoffer; Møldrup, Per; Thorndahl, Søren Liedtke; Nielsen, Jesper Ellerbæk; Duus, Lene Bassø; Rasmussen, Søren Højmark; Uggerby, Mads

*Published in:*  
Hydrological Processes

*DOI (link to publication from Publisher):*  
[10.1002/hyp.13563](https://doi.org/10.1002/hyp.13563)

*Creative Commons License*  
CC BY 4.0

*Publication date:*  
2019

*Document Version*  
Publisher's PDF, also known as Version of record

[Link to publication from Aalborg University](#)

*Citation for published version (APA):*  
Nielsen, K., Møldrup, P., Thorndahl, S. L., Nielsen, J. E., Duus, L. B., Rasmussen, S. H., & Uggerby, M. (2019). Automated rainfall simulator for variable rainfall on urban green areas. *Hydrological Processes*, 33(26), 3364-3377. <https://doi.org/10.1002/hyp.13563>

### General rights

Copyright and moral rights for the publications made accessible in the public portal are retained by the authors and/or other copyright owners and it is a condition of accessing publications that users recognise and abide by the legal requirements associated with these rights.



- ? Users may download and print one copy of any publication from the public portal for the purpose of private study or research.
- ? You may not further distribute the material or use it for any profit-making activity or commercial gain
- ? You may freely distribute the URL identifying the publication in the public portal ?

### Take down policy

If you believe that this document breaches copyright please contact us at [vbn@aub.aau.dk](mailto:vbn@aub.aau.dk) providing details, and we will remove access to the work immediately and investigate your claim.

## RESEARCH ARTICLE

# Automated rainfall simulator for variable rainfall on urban green areas

Kristoffer T. Nielsen<sup>1,4</sup>  | Per Moldrup<sup>1</sup> | Søren Thorndahl<sup>1</sup>  | Jesper E. Nielsen<sup>1</sup> | Lene B. Duus<sup>2</sup> | Søren H. Rasmussen<sup>3</sup> | Mads Uggerby<sup>4</sup> | Michael R. Rasmussen<sup>1</sup>

<sup>1</sup>Department of Civil Engineering, Aalborg University, Aalborg, Denmark

<sup>2</sup>Wastewater planning, Aarhus Vand A/S, Viby, Denmark

<sup>3</sup>Urban drainage planning, EnviDan A/S, Kastrup, Denmark

<sup>4</sup>Urban drainage planning, EnviDan A/S, Silkeborg, Denmark

## Correspondence

Kristoffer T. Nielsen, Department of Civil Engineering, Aalborg University, Thomas Manns Vej 23, 9220 Aalborg, Denmark; or EnviDan A/S, Vejlsøvej 23, 8600 Silkeborg, Denmark.  
Email: kni@civil.aau.dk

## Funding information

The Foundation for Development of Technology in the Danish Water Sector, Grant/Award Number: 7831.2015; Aalborg University; EnviDan; Aarhus Vand; Innovation Fund Denmark; Foundation for Development of Technology in the Danish Water Sector; Aalborg University; EnviDan; Aarhus Vand; Innovation Fund Denmark, Grant/Award Number: 5016-00155B; Foundation for Development of Technology in the Danish Water Sector

## Abstract

Rainfall simulators can enhance our understanding of the hydrologic processes affecting the total runoff to urban drainage systems. This knowledge can be used to improve urban drainage designs. In this study, a rainfall simulator is developed to simulate rainfall on urban green surfaces. The rainfall simulator is controlled by a microcomputer programmed to replicate the temporal variations in rainfall intensity of both historical and synthetic rainfall events with constant rainfall intensity on an area of 1 m<sup>2</sup>. The performance of the rainfall simulator is tested under laboratory conditions with regard to spatial uniformity of the rainfall, the kinetic energy of the raindrops, and the ability to replicate historical and synthetic rainfall events with temporally varying intensity. The rainfall simulator is applied in the field to evaluate its functionality under field conditions and the influence of wind on simulated rainfall. Finally, a field study is carried out on the relationship between runoff, soil volumetric water content, and surface slope. Performance and field tests show that the simulated rainfall has a uniform spatial distribution, whereas the kinetic energy of the raindrops is slightly higher than that of other comparable rainfall simulators. The rainfall simulator performs best in low wind speed conditions. The simulator performs well in replicating historical and synthetic rainfall events by matching both intensity variations and accumulated rainfall depth. The field study shows good correlation between rainfall, runoff, infiltration, soil water content, and surface slope.

## KEYWORDS

infiltration, pervious surfaces, rainfall–runoff, rainfall simulator, surface runoff, urban drainage, valve control, variable rainfall

## 1 | INTRODUCTION

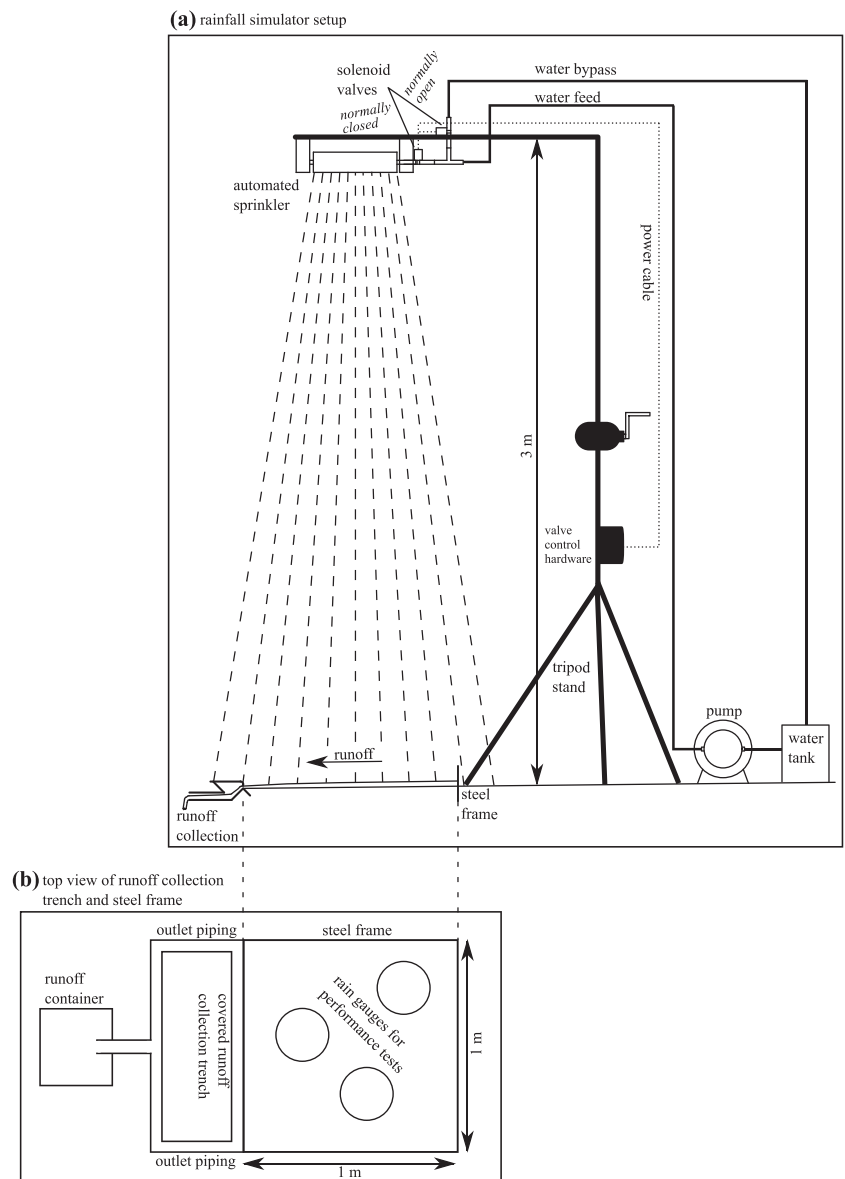
Little empirical knowledge exists on rainfall–runoff processes from urban permeable green surfaces, such as parks and gardens (Redfern, MacDonald, Kjeldsen, Miller, & Reynard, 2016). Such areas often cover more than half of the surface area in urban settings and can therefore contribute significantly to the total runoff reaching urban

drainage systems. However, the amount of runoff produced largely depends on local physical properties, such as soil type, soil saturation, vegetation cover, soil compaction, and morphological properties (Gregory, 2006; Groenendyk, Ferré, Thorp, & Rice, 2015; Quinton, Edwards, & Morgan, 1997; Sharma, 1986). These factors result in a large spatial variation in runoff generation. The hydrological rainfall–runoff mechanisms in such areas are complex. Hydrological

This is an open access article under the terms of the Creative Commons Attribution License, which permits use, distribution and reproduction in any medium, provided the original work is properly cited.

© 2019 The Authors. Hydrological Processes published by John Wiley & Sons Ltd

**FIGURE 1** Schematics of (a) the rainfall simulator setup and (b) the water collection system used for runoff monitoring. Note that the scale is not representative in this illustration



parameterization rarely relies on site-specific empirical evidence. Therefore, it is necessary to develop tools to quantify these mechanisms to improve future urban drainage design. In this way, urban drainage engineers will be able to give estimates of runoff in urban drainage modelling with greater certainty. Furthermore, experimental quantification of runoff processes from permeable green surfaces can potentially be used to calibrate traditional infiltration models in urban drainage engineering, such as Horton's infiltration equation or the Green-Ampt model (Green & Ampt, 1911; Horton, 1939).

In rural and agricultural areas, rainfall simulators are widely used to evaluate the effects of runoff on permeable surfaces. For instance, rainfall simulators have been used in nutrient transport studies (Sharpley, 2003), rainfall-runoff, and soil erosion studies (Arnaez, Lasanta, Ruiz-Flaño, & Ortigosa, 2007; Benavides Solorio & MacDonald, 2001; Burch, Moore, & Burns, 1989). Nevertheless, significantly fewer studies are found on rainfall

simulators used to assess rainfall-runoff processes in urban drainage and mitigation of torrential rain. Thus, there is a need for further developments in both large-scale experimental field stations (Nielsen et al., 2019) and rainfall simulators to study the effects of rainfall-runoff from green areas in urban drainage planning and design. This type of study will improve the understanding of the inherent processes of green area rainfall-runoff in urban hydrological systems and potentially improve urban stormwater management in the future.

Rainfall simulators are primarily divided into gravity-driven, drip-forming simulators (Clarke & Walsh, 2007) and pressure-driven simulators with spray nozzles (Humphry, 2002). Often, special emphasis is placed on replicating different physical characteristics of rain, such as spatial uniformity, rainfall intensity, raindrop size distribution, and raindrop kinetic energy (Abudí, Carmi, & Berliner, 2012; Cerdà, Ibáñez, & Calvo, 1997), whereas most rainfall simulators can produce only one or two rainfall intensity levels. Few studies have

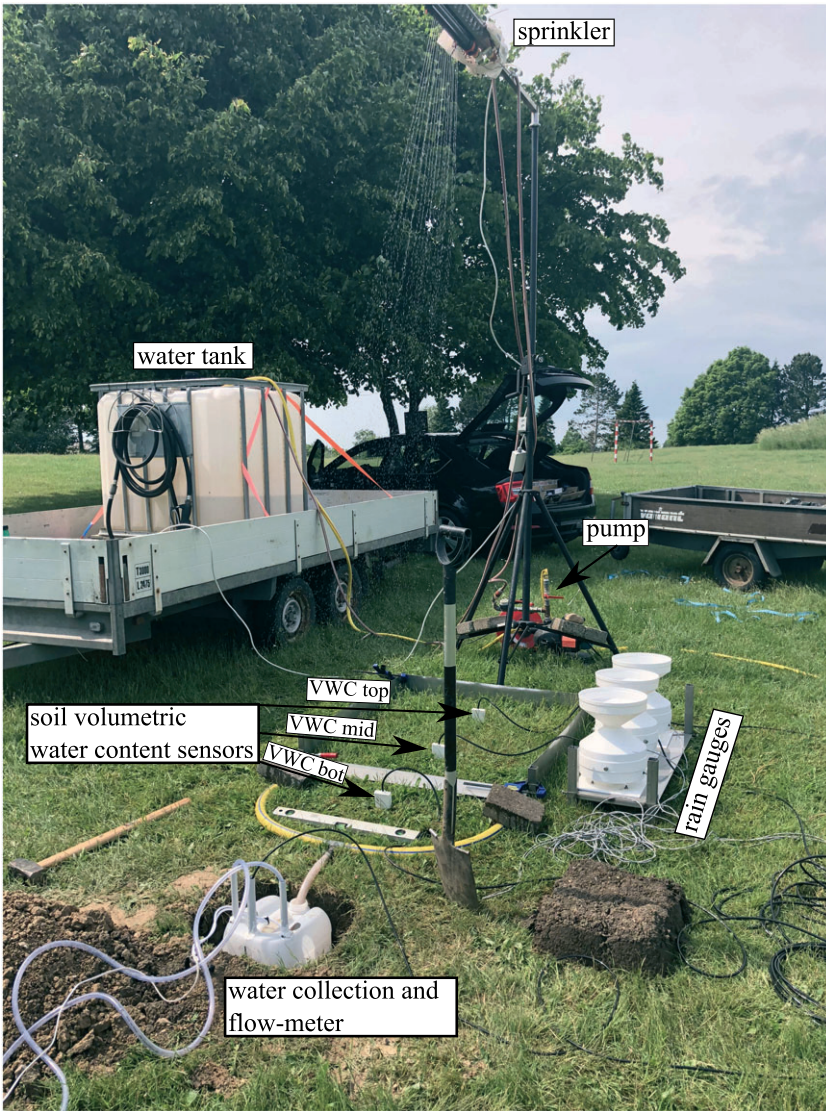


**FIGURE 2** Rainfall simulator assembled on site for field experiments. VWC top, VWC mid, and VWC bot are the locations of individual soil VWC sensors, which are placed 25, 75, and 125 cm away from the upstream steel frame boundary (closest to the tripod stand), respectively. Abbreviation: VWC, volumetric water content

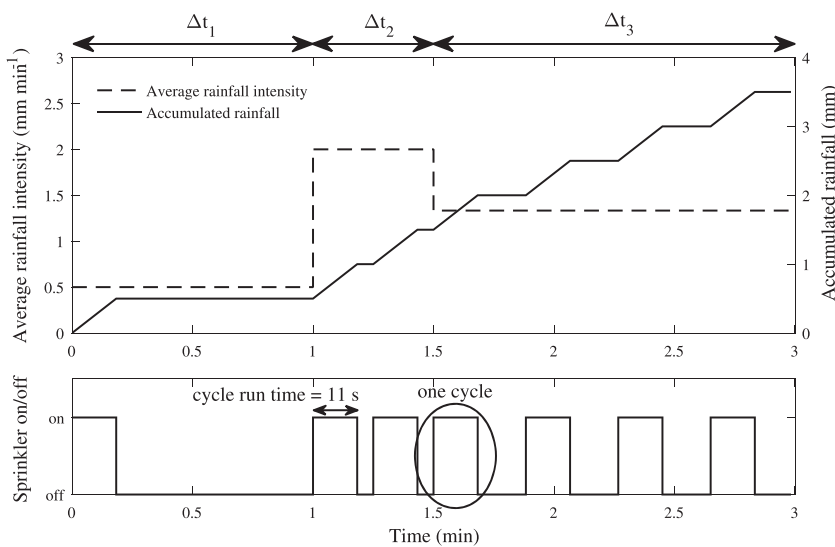


**FIGURE 3** Conceptual drawing of the process of rainfall simulation. In this drawing, it is assumed that the cycle rainfall load is 0.5 mm per cycle. The cycle run time is 11 s, which is the period during which the sprinkler is active. One active period represents one cycle

developed solenoid valve-controlled rainfall simulators to create graduated intensities (Miller, 1987; Paige, 2004). By running a solenoid valve with predefined opening/closing rates, which subsequently sets

the on/off rates of the rainfall simulator, the average amount of water applied is controlled. In doing so, it is possible to reach a varied spectrum of rainfall intensities with a single rainfall simulator and nozzle.

Paige (2004) further applied this technique to manually change the rainfall intensity during a simulation, thereby making the simulated rainfall temporally variable.

In the present work, we investigated how microcomputer-controlled solenoid valves can improve the design of an automated rainfall simulator. Herein, the rainfall simulator is designed to simulate rainfall on vegetated surfaces. The simulator must be capable of reproducing recorded historical rainfall events with both constant and varying rainfall intensities. This gives the simulator the flexibility to study a large spectrum of different rainfall types, which is critical for rainfall–runoff from urban green surfaces. The simulator is designed for a plot size of 1 m<sup>2</sup> to increase the mobility of the apparatus. Compared with larger plot sizes, the small plot size used herein will require more simulations to map the soil heterogeneity. However, this is a reasonable cost to be able to assemble and disassemble equipment faster on site. Additionally, the mobility of the small simulator will make it possible to investigate multiple surface types (e.g., different slopes, soil water content, and vegetation) within a short period of time. Designing a rainfall simulator for larger plot sizes would increase the complexity of the system in terms of the control strategies, that is, a larger plot would require several sprinklers, which would necessitate the simultaneous control of several units.

The performance of the rainfall simulator is tested under laboratory and field conditions. In the laboratory, the spatial uniformity of rainfall generated by the simulator is determined, along with

how well the simulator can replicate historical rainfall events with variable intensity. Finally, the kinetic energy of the raindrops is measured under laboratory conditions. Field performance tests of the simulator are combined with an extended field campaign with constant rainfall intensity. In the field testing phase, a system developed for water collection, runoff estimation, and soil water content measurement is evaluated. The extended field campaign investigates whether relationships between runoff, infiltration, soil water content, and surface slope can be derived on the basis of simulated rainfall. These results are used to assess the suitability of rainfall simulators as a tool for risk assessment of rainfall–runoff from urban green areas.

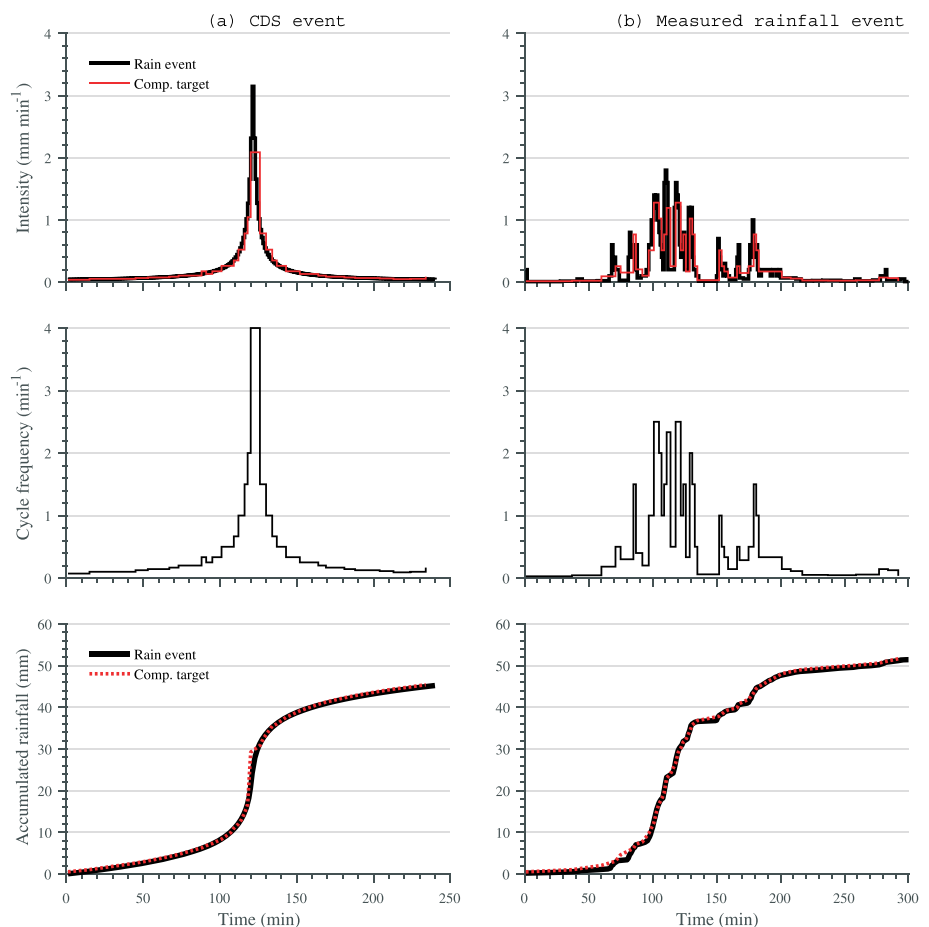
The primary objective of this study is to present a method for urban drainage engineers to quantify rainfall infiltration under various physical conditions. This method will be helpful in estimating the risk of runoff from urban green areas under different physical conditions, including soil water content and surface slope. Additionally, the developed rainfall simulator presents a method to investigate several types of rainfall with a single simulator.

## 2 | MATERIALS AND METHODS

### 2.1 | Materials

The rainfall simulator system outlined in Figure 1a consists of six main components: (a) an automated sprinkler to generate and

**FIGURE 4** Conservation in (a) a Chicago design storm (CDS; Keifer & Chu, 1957) with a return period of 30 years and (b) a measured rainfall event. The measured rainfall event was recorded north of Aarhus, Denmark (Lat, Long, Alt = 56.21, 10.24, 1), during August 26, 2012. The computed target lines are the fitted rain events that become the target value and input for the rainfall simulation by the algorithm. Temporally variable rainfall intensity, accumulated rainfall, and cycle frequency are illustrated. The cycle frequency represents the number of cycles that runs on average each minute. The cycle frequency is fitted with a cycle rainfall load of 0.522 and 0.511 mm per cycle





distribute water droplets, (b) a tripod to elevate the sprinkler with an adjustable height of up to 3 m, (c) a pump to supply the system with water from a tank, (d) two solenoid valves to regulate the flow of the system, (e) a programmable microcontroller, and (f) a water tank supplying the system with water. In this case, the sprinkler is raised to an elevation of 3 m. This elevation distributes the water drops uniformly over the 1 m × 1 m measurement surface area on the ground. A Gardena® pump 3000/4 supplies the water, and the sprinkler is a commercially available Gardena Aquazoom® oscillating sprinkler that forms a one-dimensional arc boom. When applying water, the sprinkler oscillates sideways and waters a plane. The system always needs to be pressurized to avoid air entry through the sprinkler, as air in the system can disturb the smooth operation of the automated sprinkler. The water supply to the sprinkler is regulated by two solenoid valves, which can switch the water flow on and off by electromagnetic induction. The primary valve opens and closes the water supply to the sprinkler, whereas the secondary bypass valve ensures a recirculation of the water flow when the primary valve is closed. The solenoid valves are operated with time-dependent open/close frequency to achieve the desired average rainfall intensity over the desired time interval. An Arduino® Uno controls the open/close routine of the solenoid valves with an ATmega328P microprocessor using a relay connecting the solenoid valves with a 12-V battery.

In the field experiments, generated runoff is collected from a 1 m<sup>2</sup> surface (1 m × 1 m) in the water collection system illustrated in Figure 1b. The water collection system consists of three main components: (a) a three-sided steel frame preventing surface runoff from exiting or entering the measurement area, (b) a fourth side consisting of a steel trench (the downstream side) that collects runoff and directs it through pipes to a runoff container, and (c) a runoff container that collects the runoff and is used to estimate the flow rate by measuring the change in the water level with a Campbell Scientific CS451 pressure transducer (Campbell Scientific, 2014). Two small submerged 12-V pumps are installed in the runoff container for drainage.

During field experiments, three Campbell Scientific CS655 soil volumetric water content (VWC) sensors (Campbell Scientific, 2018) are used to measure the water content of the soil from 0 to 12 cm of depth. These sensors are inserted 25, 75, and 125 cm from the upper steel frame boundary (steel frame side closest to the tripod in Figures 1a and 2); these sensors are denoted as "VWC top," "VWC mid," and "VWC bot," respectively. Two sensors are located within the measurement area, whereas one is located outside at the downstream boundary of the measurement area to monitor if any flow towards this point is present in the soil.

## 2.2 | Rainfall generation method

The automated sprinkler runs in cycles as illustrated in Figure 3. One cycle consists of the sprinkler boom moving forth and back once. One cycle always takes 11 s, as indicated by the "cycle run time" in Figure 3. The rainfall simulator is applying rainfall only to the area of interest in this duration. The average applied rainfall during one cycle (cycle rainfall load) is determined by calibration with rain gauges.

Figure 3 shows that the average rainfall intensity will increase as the cycles occur more frequently, and the intensity is calculated as follows:

$$I_{avg,i} = \frac{1}{\Delta t_i} (P_{cycle} n_{cycle,i}), \quad (1)$$

where  $I_{avg,i}$  (mm min<sup>-1</sup>) is the average rainfall intensity,  $\Delta t_i$  (min) is the time interval,  $P_{cycle}$  (millimetres per cycle) is the cycle rainfall load, and  $n_{cycle,i}$  (cycle) is the number of cycles within the time interval.

An algorithm is developed to adjust the cycle frequency so that the simulated rainfall volume reaches the rainfall volume of either a recorded historical rainfall event or a synthetic rainfall event. This means that if there is a need for a higher rainfall intensity within a certain time frame, the cycle frequency is increased to increase the average rainfall intensity within that time frame. In time frames with lower rainfall intensities, the cycle frequency is decreased. It is important to note that the cyclic operation of the rainfall simulator means that the applied rainfall intensity during the cycle does not change. The result of this approach is that during a time frame with low rainfall intensity (low cycle frequency of the rainfall simulator), there are periods with a significantly higher rainfall intensity (i.e., when the rainfall simulator is active during the cycles). Therefore, this approach might not be suitable for erosion, nutrient, or contaminant transport studies but solely studies related to rainfall infiltration.

The cycle rainfall load is dependent on the physical setup of the system, clogging of filters, and/or other factors influencing pressure loss in the system. Thus, calibration of the cycle rainfall load is required and is estimated to be 0.55 mm per cycle. Consequently, the maximum rainfall intensity that the rainfall simulator can produce is approximately 2.75 mm min<sup>-1</sup>, as a maximum of five cycles can be achieved within 1 min.

The developed algorithm seeks to guarantee good conservation of rainfall depth. The algorithm divides the input rainfall event (either recorded or synthetic rainfall event) into variable time intervals,  $\Delta t_i$ , as shown in Figure 3. In this way, both the time interval and cycle frequency can be adjusted. For example, if adding another cycle within a time interval would add an excessive amount of rainfall, the time interval can be shortened slightly instead.

When mass conservation with the derived average rainfall intensity and time interval is acceptable, the algorithm proceeds to define the next variable time interval. This approach results in flexible time intervals with varying cycle frequencies, as illustrated for a synthetic Chicago design storm (Keifer & Chu, 1957; Madsen, Gregersen, Rosbjerg, & Arnbjerg-Nielsen, 2017) and a recorded variable rainfall event in Figure 4a,b. The computed targets in Figure 4a,b are the rainfall intensities and accumulated rainfall depths calculated by the algorithm shown in Figure 3. If a rainfall event with a uniform rainfall intensity had been used instead, the cycle frequency would have been constant throughout the entire event.

The cycle frequency plotted in the middle row of Figure 4 is the input to the microcomputer, which controls the rainfall simulator. Ideally, the computed cycle frequency should result in a rainfall event

depth that matches the target event. However, because the cycle rainfall load is constant and the cycle run time of the sprinkler is 11 s, minor deviations cannot be avoided. For the events shown in Figure 4, the event rainfall depth of the computed target deviates 0.42% for the replicated event (Figure 4a) and 0.08% for the replicated event (Figure 4b).

### 2.3 | Laboratory tests

The performance of the rainfall simulator is evaluated under laboratory conditions, wherein it is determined whether the simulator can distribute the simulated rainfall spatially uniformly onto the area of interest. The kinetic energy of the raindrops is measured to ensure that the simulator does not possess any extreme levels of kinetic energy. Finally, the ability of the simulator to replicate recorded and synthetic rainfall events are evaluated against three tipping bucket gauges.

The ability of the rainfall simulator to provide a uniform spatial distribution of rainfall is evaluated by Christiansen's coefficient of uniformity (Christiansen, 1942):

$$C_u = 100 \left( 1 - \frac{\sum x}{mn} \right), \quad (2)$$

where  $C_u$  (-) is Christiansen's coefficient of uniformity,  $x$  (ml) is the deviation of individual observations from the mean value,  $m$  (millilitres per observation) is the mean value of observations, and  $n$  (obs) is the number of observations. Uniformity is measured in 24 foil trays covering an area of 17.5 cm × 22 cm each. The 24 foil trays are set up in a 6 × 4 grid, covering 88% of the 1 m<sup>2</sup> area of interest (1 m × 1 m). Thus, the measurements in the foil trays are representative of the uniformity upon the entire area. The collected water in the foil trays is then weighed to measure the contained rainfall volume.

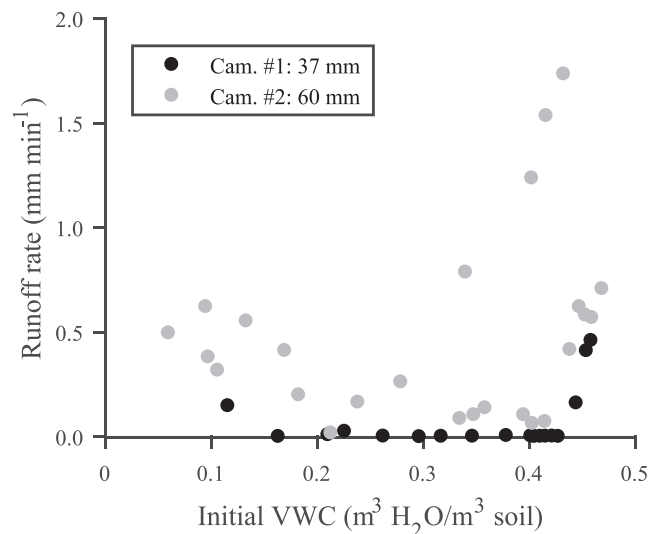


**FIGURE 6** Correlation between the initial soil volumetric water content (VWC) and the average runoff rate from 43 rainfall simulations. Cam. #1 presents the collected data of the 18 field performance tests applying 37 mm of rainfall for 30 min. Cam. #2 presents the collected data of the 25 extended rainfall simulation field campaigns applying 60 mm of rainfall for 30 min

The rainfall simulator is not designed for soil erosion studies; the simulator is intended only for simulation on vegetated surfaces where erosion is expected to be minimal. However, this study still investigates whether the simulator has any extreme behaviour in terms of the kinetic energy of simulated raindrops. The kinetic energy is derived from the raindrop size distribution and raindrop velocity and is measured with an OTT Parsivel<sup>2</sup> disdrometer (Bartholomew, 2014; OTT Hydromet, 2011). The kinetic energy is determined by the mass and travelling speed of the raindrops. This approach is commonly used

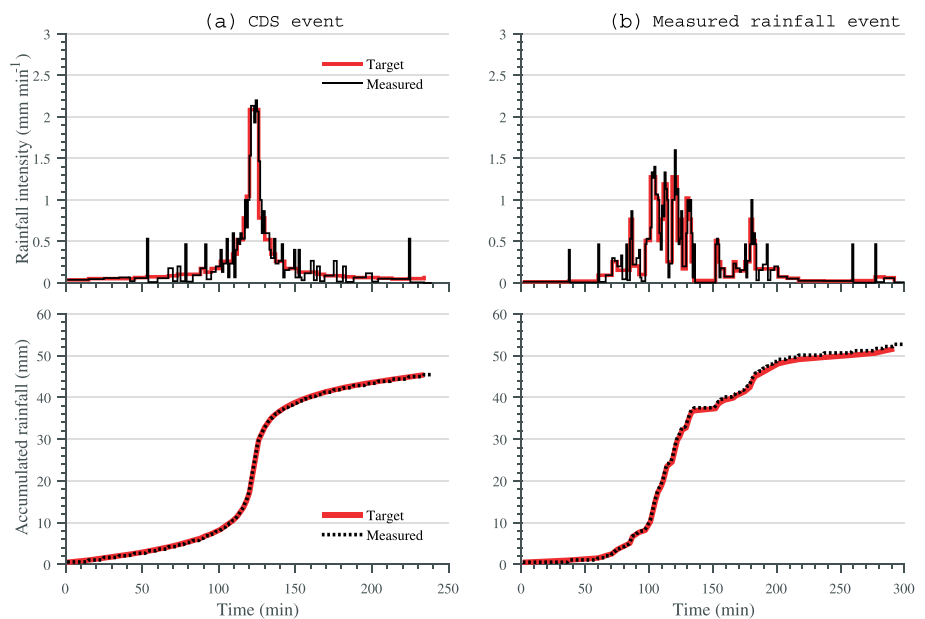


**FIGURE 5** Comparison of the measured rainfall based on the average of the three tipping bucket gauges illustrated in Figure 1 to the computed target values in Figure 4. The rainfall intensity and average accumulated rainfall are illustrated comparatively with the computed target. Abbreviation: CDS, Chicago design storm

**TABLE 1** General experimental data and results from rainfall simulations carried out in the field tests (FT1–FT18) and extended field campaigns (ESC1–ESC25)

Rainfall simulation data								
	Surface slope	Acc. rainfall	Average rainfall intensity	Initial VWC	Mean VWC	Acc. runoff	Average runoff rate	Average infiltration rate
	(%)	(mm)	(mm min <sup>-1</sup> )	(m <sup>3</sup> H <sub>2</sub> O/m <sup>3</sup> soil)	(m <sup>3</sup> H <sub>2</sub> O/m <sup>3</sup> soil)	(mm)	(mm min <sup>-1</sup> )	(mm min <sup>-1</sup> )
FT1	0.14	37	1.23	0.12	0.20	4.41	0.15	1.09
FT2	0.14	37	1.23	0.23	0.25	0.74	0.02	NV <sup>a</sup>
FT3	0.14	37	1.23	0.26	0.29	0.05	0.00	NV
FT4	0.14	37	1.23	0.30	0.33	-0.03 <sup>b</sup>	0.00	NV
FT5	0.14	37	1.23	0.35	0.38	0.03	0.00	NV
FT6	0.06	37	1.23	0.16	0.25	0.00	0.00	NV
FT7	0.06	37	1.23	0.32	0.38	0.02	0.00	NV
FT8	0.06	37	1.23	0.41	0.43	0.00	0.00	NV
FT9	0.06	37	1.23	0.44	0.45	4.81	0.16	1.07
FT10	0.06	37	1.23	0.45	0.46	12.30	0.41	0.82
FT11	0.06	37	1.23	0.46	0.39	13.77	0.46	0.77
FT12	0.10	37	1.23	0.21	0.32	0.24	0.01	NV
FT13	0.10	37	1.23	0.38	0.40	0.13	0.00	NV
FT14	0.10	37	1.23	0.40	0.41	0.08	0.00	NV
FT15	0.10	37	1.23	0.41	0.42	0.02	0.00	NV
FT16	0.10	37	1.23	0.42	0.42	0.03	0.00	NV
FT17	0.10	37	1.23	0.42	0.43	0.05	0.00	NV
FT18	0.10	37	1.23	0.43	0.43	0.01	0.00	NV
ESC1	0.12	60	2.00	0.11	0.16	9.50	0.32	1.69
ESC2	0.12	60	2.00	0.18	0.24	5.97	0.20	1.81
ESC3	0.12	60	2.00	0.28	0.37	7.83	0.26	1.75
ESC4	0.11	60	2.00	0.10	0.12	18.62	0.62	1.38
ESC5	0.11	60	2.00	0.13	0.16	16.57	0.55	1.45
ESC6	0.11	60	2.00	0.17	0.29	12.33	0.41	1.59
ESC7	0.11	60	2.00	0.34	0.39	23.58	0.79	1.21
ESC8	0.11	60	2.00	0.40	0.42	37.07	1.24	0.76
ESC9	0.11	60	2.00	0.42	0.43	46.01	1.53	0.46
ESC10	0.11	60	2.00	0.43	0.44	52.00	1.73	0.26
ESC11	0.07	60	2.00	0.10	0.15	11.40	0.38	1.62
ESC12	0.07	60	2.00	0.21	0.30	0.50	0.02	1.99
ESC13	0.07	60	2.00	0.34	0.42	2.58	0.09	1.92
ESC14	0.07	60	2.00	0.44	0.46	12.47	0.42	1.59
ESC15	0.07	60	2.00	0.45	0.47	17.41	0.58	1.42
ESC16	0.07	60	2.00	0.46	0.47	17.06	0.57	1.44
ESC17	0.07	60	2.00	0.45	0.47	18.61	0.62	1.38
ESC18	0.07	60	2.00	0.47	0.47	21.20	0.71	1.30
ESC19	0.09	60	2.00	0.06	0.16	14.85	0.50	1.50
ESC20	0.09	60	2.00	0.24	0.33	4.93	0.16	1.83
ESC21	0.09	60	2.00	0.35	0.39	3.11	0.10	1.89
ESC22	0.09	60	2.00	0.36	0.41	4.11	0.14	1.86
ESC23	0.09	60	2.00	0.40	0.42	3.12	0.10	1.89

(Continues)



**TABLE 1** (Continued)

Rainfall simulation data								
	Surface slope	Acc. rainfall	Average rainfall intensity	Initial VWC (m <sup>3</sup> H <sub>2</sub> O/m <sup>3</sup> soil)	Mean VWC (m <sup>3</sup> H <sub>2</sub> O/m <sup>3</sup> soil)	Acc. runoff	Average runoff rate	Average infiltration rate
	(%)	(mm)	(mm min <sup>-1</sup> )			(mm)	(mm min <sup>-1</sup> )	(mm min <sup>-1</sup> )
ESC24	0.09	60	2.00	0.40	0.43	1.87	0.06	1.93
ESC25	0.09	60	2.00	0.42	0.43	2.14	0.07	1.93

Abbreviation: VWC, volumetric water content.

<sup>a</sup>NV means that no value of the average infiltration rate is calculated as produced runoff is minimal.

<sup>b</sup>Small negative value is due to either minor measurement error or temporary fluctuations in the runoff collection tank.

in rainfall simulator studies on soil erosion (Abudi et al., 2012; Gilley & Finkner, 1985):

$$E_{kin} = \frac{1}{2} I \sum_i m_i v_i^2, \quad (3)$$

where  $E_{kin}$  (J m<sup>-2</sup> m<sup>-1</sup>) is the kinetic energy of the raindrop spectrum,  $I$  (m s<sup>-1</sup>) is the intensity of the rainfall,  $m_i$  (kg) is the mass of the raindrops in each size group, and  $v_i$  (m s<sup>-1</sup>) is the travelling velocity of the raindrops in each size group.

The event replication performance of the system is evaluated by simulating the computed target rainfall in Figure 4a,b and measuring the simulated rainfall via three ARG100 tipping bucket rain gauges with tipping bucket volumes of 0.2 mm per tip with 1-min logging intervals (Campbell Scientific, 2010) located within 1 m<sup>2</sup>, as illustrated in Figure 1. The ability of the rainfall simulator to achieve good rainfall depth conservation in comparison with the computed target rainfall in Figure 4 is evaluated.

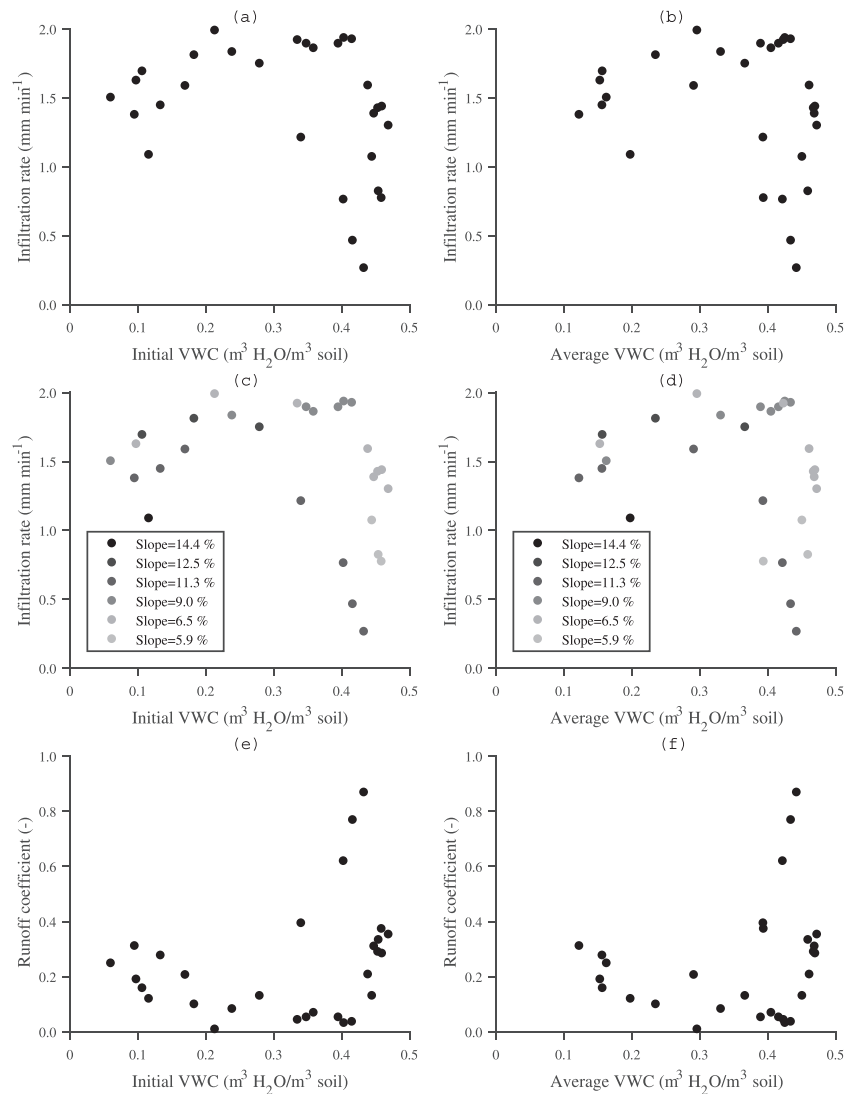


**FIGURE 7** Correlations between the initial soil volumetric water content (VWC) and the (a) infiltration rate, (c) surface slope, and (e) runoff coefficient. Correlations between the average soil VWC and the (b) infiltration rate, (d) surface slope, and (f) runoff coefficient

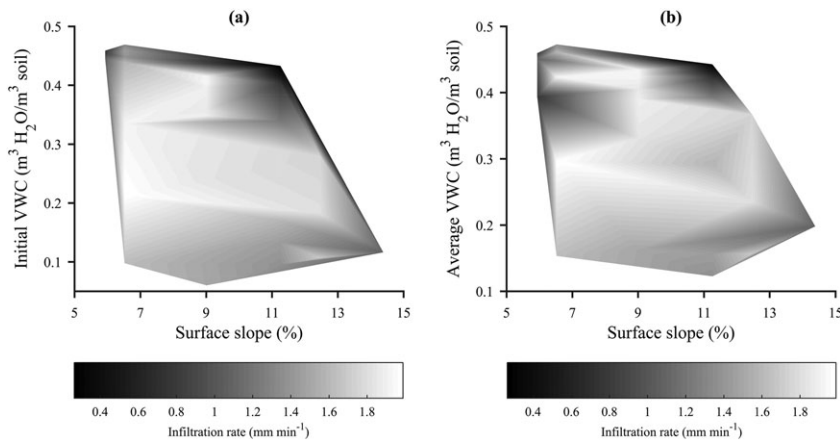


**FIGURE 8** (a) Three-dimensional relationship between the infiltration rate, initial soil volumetric water content (VWC), and surface slope. (b) Three-dimensional relationship between the infiltration rate, average soil VWC, and surface slope

## 2.4 | Field performance test simulations

Field performance tests are conducted under near optimal conditions regarding minor wind disturbances, constant water level in the reservoir, and optimal conditions for setting up the equipment. A total of 18 field test replicates were made with constant rainfall on surfaces with three different slopes and varying initial soil water content conditions. The surfaces are covered in grass, and the soil is classified as a sandy loam soil according to the U.S. Department of Agriculture soil classification system (Ashman & Puri, 2013). In this way, it is possible to investigate whether external variables could influence the performance of the rainfall simulator. The study site is located in Lystrup, Denmark, and has previously been studied in terms of runoff processes occurring in field scale under natural rainfall and soil conditions (Nielsen et al., 2019). An accumulated rainfall depth of 37 mm is added uniformly for 30 min, corresponding to a 100-year event for this area (Madsen et al., 2017).

## 2.5 | Extended rainfall simulation campaign

In addition to the 18 field tests, an extended field campaign with 25 field experiments was conducted in the same area. Not all 18 field tests produced runoff; therefore, an accumulated rainfall depth of 60 mm was added uniformly for 30 min for the experimental field campaign. Rainfall with constant rainfall intensity is used to maximize the entry of water into the soil pore space and to ensure the same initial conditions. Data collected throughout the experimental field

campaign are combined with data from the field test of the rainfall simulator. The experimental field campaign studies the relationship between the initial and average soil VWC compared with the average infiltration rate, slope, and runoff coefficient. The average infiltration rate in a simulation is estimated on the basis of the average rainfall intensity combined with the average runoff rate. Additionally, the relationship between the initial soil VWC, the time before the initiation of runoff, and the initial loss is assessed by analysing the time elapsed before runoff starts (i.e., before runoff is monitored in the runoff container).

## 3 | RESULTS

### 3.1 | Laboratory tests

Christiansen's coefficient of uniformity is investigated in five separate tests applying an average cycle load of 0.56 mm per cycle and an average total rainfall depth of 13.9 mm uniformly over 6.3 min; this corresponds to 25 cycles in each test. An average  $C_u$  of  $95.3\% \pm 1.7\%$  was found. Additionally, it was found that the average percentage deviation from the mean rain depth at each observation point ranged between  $-7.1\%$  and  $12.8\%$ . Hence, it is concluded that the uniformity of the sprinkler is satisfactory.

The raindrop size and velocity distribution from 10 disdrometer tests showed an average applied kinetic energy of  $34.9 \text{ J m}^{-2} \text{ mm}^{-1}$ . Each test had 40 cycles uniformly distributed over 10 min. Regardless

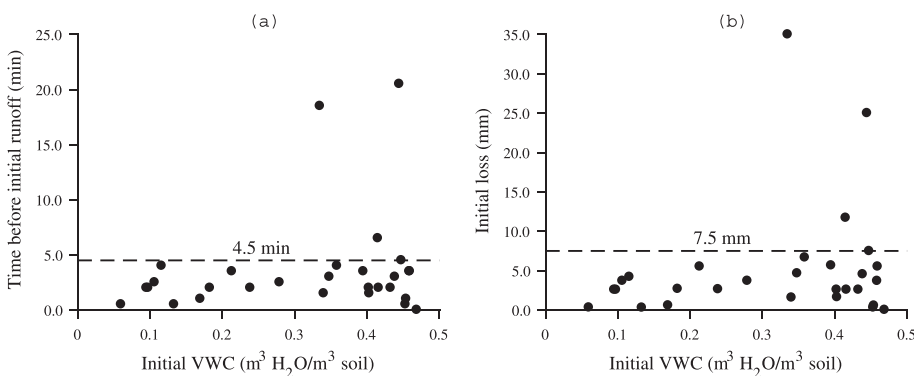
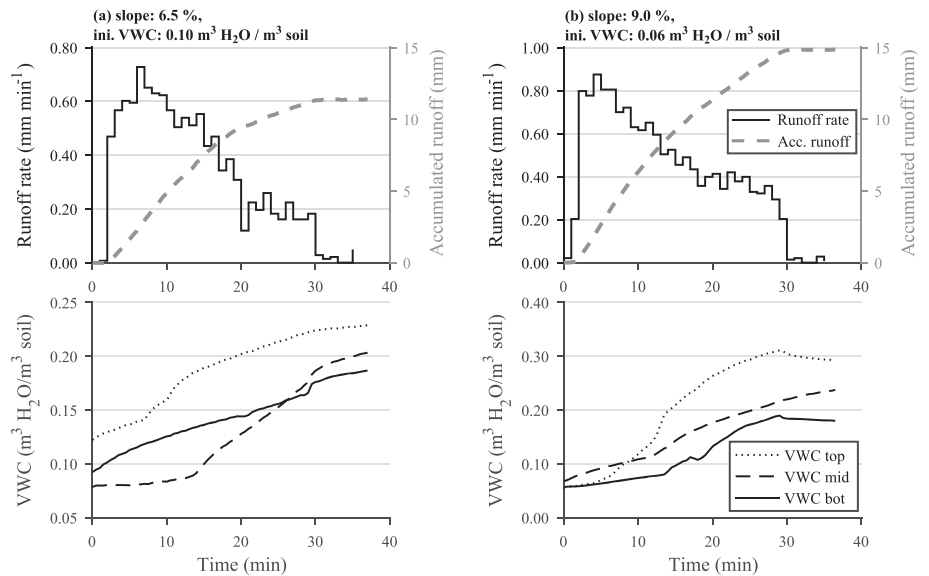


**FIGURE 9** Correlation between initial soil volumetric water content (VWC) and (a) the time before initial runoff is recorded during rainfall simulation and (b) the initial loss within the periods before runoff is initiated

**FIGURE 10** Two rainfall simulator tests showing the effects of soil water repellence under low soil water content conditions on generated runoff from two measurement plots of 1 m<sup>2</sup>. Note that 60 mm of rainfall was applied over 30 min. The soil volumetric water content (VWC) was measured with three soil water content sensors, as shown in Figure 2



of the rainfall intensity, the applied kinetic energy is fixed due to the cyclic behaviour of the rainfall simulator.

In Figure 5, the measured output from the rainfall simulator is compared with the computed target input (Figure 4). It appears that the average measured accumulated rainfall volumes are almost identical to the target. The measured total accumulated rainfall deviates from the target values by 0.09% to 2.11%. This demonstrates that the rainfall simulator operation is stable and is reliable during events of up to at least 5 hr. Small fluctuations are visible in the measured intensity in Figure 5; however, these fluctuations are likely due to the measurement method of tipping bucket gauges logging the number of tips each minute.

### 3.2 | Field performance test simulations

Figure 6 illustrates the results of the 18 field tests presented in Table 1 by applying 37 mm of rainfall within 30 min onto three different surface slopes. Only four simulations during the field test resulted in significant amounts of runoff. The remaining simulations produced practically no runoff as the infiltration capacity was larger than the applied rainfall intensity. Runoff was only recorded at initial soil VWCs either less than 0.13 or greater than 0.43 m<sup>3</sup> H<sub>2</sub>O/m<sup>3</sup> soil, as shown in Figure 6. Soil water contents between 0.13 and 0.43 m<sup>3</sup> H<sub>2</sub>O/m<sup>3</sup> soil did not produce runoff. This means that these simulations cannot be used for estimation of the infiltration capacity in this case because it is higher than the applied rainfall intensity. Finally, it was observed at the site that wind significantly affects the rainfall simulations, as gusty winds were able to blow the droplets outside the intended measurement area.

### 3.3 | Extended rainfall simulation campaign

Combining the field performance tests and the extended rainfall simulation campaign presented in Figure 6 and Table 1, it is possible to obtain a well-defined relationship between different soil water

content conditions and infiltration. Figure 6 shows that rainfall simulations producing no runoff are excluded. The remaining simulations are presented in Figure 7a,b, where the infiltration rate is compared with the initial and average soil VWC of each rainfall simulation. Figure 7a, b shows that both the initial and average soil water content are strongly correlated with the infiltration rate. Generally, the infiltration rate is relatively low at an initial soil VWC between 0.06 and 0.17 m<sup>3</sup> H<sub>2</sub>O/m<sup>3</sup> soil, resulting in infiltration rates between 1.1 and 1.7 mm min<sup>-1</sup>. Between soil water contents of 0.17 to 0.40 m<sup>3</sup> H<sub>2</sub>O/m<sup>3</sup> soil, the infiltration rate increases to between 1.7 and 2.0 mm min<sup>-1</sup>. Finally, as the initial soil water content exceeds 0.40 m<sup>3</sup> H<sub>2</sub>O/m<sup>3</sup> soil, the infiltration rate shows greater variation. Within this interval, the infiltration rates vary between 0.3 and 1.9 mm min<sup>-1</sup>.

According to Figure 7c,d, the surface slope also seems to affect the infiltration rate. Generally, the steepest slopes have the lowest infiltration rate as more surface water effectively discharges from the surface. Additionally, steeper slopes require a lower soil VWC to have a low infiltration rate. This finding is further illustrated in Figure 8, where the three-dimensional relationship between infiltration rate, soil VWC, and slope generally shows a pattern where a combination of steep surface slope and high soil VWC results in the lowest infiltration rates. Steep slopes also seem to slightly reduce the infiltration capacity at low soil water contents. The initial soil water content in Figure 8a seems to produce a better relationship in combination with slope to estimate the infiltration rate compared with the average soil water content in Figure 8b. Note that local infiltration minima and maxima are seen in the infiltration rates in Figure 8 due to local variations in measured infiltration.

Figure 7e,f shows that the runoff coefficient mainly varies between 0 and 0.4. The highest runoff coefficients are present under either very dry or very wet soil conditions, which again is strongly correlated with low infiltration capacity under the same soil conditions. Few measurements show runoff coefficients greater than 0.40 and occur only at near-saturated soil with water contents greater than 0.40 m<sup>3</sup> H<sub>2</sub>O/m<sup>3</sup> soil.

Figure 9a shows that the time delay from the start of rainfall simulation to observed runoff does not correlate with the initial soil water content. The delay before runoff inception from 1 m<sup>2</sup> lies primarily between 0 and 4.5 min. Only a few measurements show significantly longer delays that are greater than 4.5 min. The reason for this finding is that the infiltration capacity of the surface is not immediately exceeded. By accumulating the applied rainfall before runoff inception, the initial loss including initially infiltrated rainfall is found. Figure 9b shows that the initial loss is unchanged regardless of the initial soil water content and ranges between 0 and 7.5 mm, including initial infiltration.

Figure 10a,b presents two experiments on soil surfaces that were prone to a long dry weather period prior to the simulation. Both experiments show the dynamics of how the water content conditions influence the infiltration and subsequently the runoff rate during the rainfall simulation. Both runoffs start with a short delay of a few minutes and with a relatively high runoff rate of 0.6 to 0.8 mm min<sup>-1</sup>. However, as the soil becomes more saturated, the infiltration rate increases, resulting in a reduced runoff rate of 0.2 to 0.4 mm min<sup>-1</sup> at the end of the 30 min of rainfall simulation.

## 4 | DISCUSSION

### 4.1 | Laboratory tests

The developed rainfall simulator performs well. The average measured Christiansen's coefficient of uniformity ( $C_u = 95.3\%$ ) is satisfying compared with a broad spectrum of rainfall simulators, which have varying values of  $C_u$  from 60.6% to 97.8% (Iserloh et al., 2013). The kinetic energy of this rainfall simulator (34.9 J m<sup>-2</sup> mm<sup>-1</sup>) is slightly larger than that of other rainfall simulators, which typically have values varying from 0.77 to 27.5 J m<sup>-2</sup> mm<sup>-1</sup> (Abudi et al., 2012; Iserloh et al., 2013) but also have values as large as 50.3 J m<sup>-2</sup> mm<sup>-1</sup> (Iserloh et al., 2013). However, the kinetic energy still falls within the natural interval for rainfall according to the review of rainfall intensity–kinetic energy relationships by Van Dijk, Bruijnzeel, and Rosewell (2002), who reported kinetic energy values from 0 to 40 J m<sup>-2</sup> mm<sup>-1</sup>. However, it must be noted that this rainfall simulator is solely developed for use in infiltration and rainfall–runoff studies on green vegetated areas and not for soil erosion studies. Substantial erosion is unlikely to happen on these kinds of surfaces, as demonstrated in the investigations by Adekalu, Olorunfemi, and Osunbitan (2007) and Pan and Shangguan (2006). Here, it was found that erosion on grass-covered surfaces is 81% to 95% less than that on bare soils.

The rainfall simulator can replicate recorded and synthetic rainfall events regarding both intensity variations and rain depth. However, there are limitations that the simulator cannot overcome. First, the rainfall simulator cannot, in its current configuration, reach rainfall intensities higher than approximately 2.75 mm within 1 min. Therefore, higher rainfall intensities are simulated with the maximum rainfall intensity of the system in a slightly longer period during the event to secure the optimal conservation of the rain depth. The impact on the

runoff study is expected to be minimal due to the integrated nature of the runoff process. However, if needed, the maximum intensity of the system can be increased by installing additional sprinkler heads. Second, there is a risk that air can enter the sprinkling funnels at very low intensities due to long idle periods between sprinkling cycles, which would cause the sprinklers to drip. However, it is unlikely that this phenomenon will significantly affect the runoff study.

Generally, the developed rainfall simulator presents a well-performing method of controlling rainfall to simulate any type of rainfall with a single simulator. Furthermore, the simulator can automatically vary the intensity during simulation with high precision. This gives an opportunity to simulate measured dynamic rainfall events and replicate these events in certain pervious areas. Therefore, this study presents a rainfall simulator that is simple to construct, performs well in terms of distributing rainfall and gives a high flexibility in terms of varying the rainfall intensity.

### 4.2 | Field performance test simulations

Field tests show that if the objective is to estimate the infiltration rate, it is necessary that the applied rainfall intensity is higher than the saturated hydraulic conductivity. However, it is only possible to evaluate the surface properties concerning runoff and infiltration in situations where runoff is produced. This could lead to a waste of valuable field time using a rainfall intensity that is smaller than the highest hydraulic conductivity. Furthermore, experience from field tests shows that wind disturbance is a significant challenge for carrying out field experiments. Visual observations showed that wind could interfere with falling raindrops and move them outside the measurement area. In severe cases, this phenomenon could lead to less rainfall being applied to the measurement area. However, this disturbance can be eliminated by installing wind barriers around the rainfall simulator.

### 4.3 | Extended rainfall simulation campaign

By increasing the rainfall intensity in the extended experimental field campaign, it was possible to increase the number of rainfall simulations that produced runoff. This provided data for a detailed analysis of the relationship between infiltration and soil VWC. The analysis shows a large variation in the infiltration rate, which ranged between 0.3 and 1.9 mm min<sup>-1</sup> depending on the soil VWC. This finding emphasizes the uncertainty associated with rainfall–runoff modelling in urban drainage engineering and the importance of correctly estimating the present soil water content when quantifying surface runoff from permeable areas. Otherwise, there is a risk of faulty estimation of surface runoff that could compromise the quality of urban drainage design.

The runoff coefficient indicates the amount of rainfall that effectively discharges from a surface and is a commonly used parameter in urban drainage engineering. This study shows that the runoff coefficient is highly dependent on the soil VWC because of its inherent link to infiltration (Figure 7e,f). Therefore, the runoff coefficient cannot be

assumed to be constant for green surfaces in the urban environment unless constant soil water conditions are present. This would only be a correct assumption under fully saturated soil conditions.

Two rainfall simulations presented in Figure 10a,b demonstrate the effects of soil water repellence of very dry topsoil. Surface runoff is triggered almost immediately after the simulations are started because of the low unsaturated hydraulic conductivity of the topsoil (Dane & Topp, 2002). This is a well-known phenomenon that is often observed in dry topsoil with high organic matter content (de Jonge, Jacobsen, & Moldrup, 1999). However, when the soil becomes wet, the effects of soil water repellence decline as the hydraulic conductivity increases significantly, thereby also increasing the infiltration capacity. This phenomenon can also be observed in Figure 10a,b, as the surface runoff rate in both cases decreases, although the applied simulated rainfall is constant during the experiments. Last, Figure 10a,b demonstrates that uneven wetting of the topsoil occurs, although the rainfall is evenly distributed. This is evident from the measured soil VWC (VWC) presented in Figure 10a, b. The soil water content increases at all locations, but the timing and the rate of increase differ. In some locations, the soil water content increases rapidly, whereas in other locations, the soil water content increases more slowly. This difference is most likely due to a different local presence of macropores on very small scales. Generally, the macropores are larger pores that transport water faster into the soil matrix.

The infiltration rates found in this study are the result of the interaction between the soil and the soil surface. In this way, surface properties also influence the estimated infiltration capacity. Steeper slopes will force water to move faster on the surface, which also indicates that less water can be retained on the surface for infiltration. Additionally, grass cover and its root system could potentially affect measured runoff, as shown by Pan and Shangguan (2006), where grass cover is found to reduce runoff compared with bare soil. Consequently, the infiltration rates found in this study are the result of both the physical characteristics of the soil and the soil surface.

#### 4.4 | Limitations of small-scale field experiments

The use of rainfall simulators primarily on small scales can result in differences when results are scaled to larger areas. Nielsen et al. (2019) developed a large-scale experimental field station that shows that subsurface throughflow is dominant during fall and winter due to horizontal mobilization of the water in the topsoil of a 4,300 m<sup>2</sup> catchment. Furthermore, the infiltration capacity of the entire catchment seems to be significantly lower than the infiltration capacities found in this study, although the simulation is carried out at the exact same location. The reason for this difference is that during fall and winter, the soil of the entire catchment has a high soil water content, and the lower soil layers seem to affect the infiltration capacity under such soil water content levels as rainfall can no longer be stored in the topsoil. This finding indicates that it is not possible to saturate the topsoil of the entire catchment and that there is sufficient storage volume in the surrounding soil of the measurement plot of the rainfall

simulator to store infiltrated simulated rainfall. Therefore, lower soil layers cannot limit the infiltration capacity in these cases. The risk of subsurface throughflow must therefore be carefully considered when characterizing the potential runoff processes in different catchments, as this is most likely an effect seen on larger scales. Therefore, the main benefit of the rainfall simulator is to compare different locations and the effects of different initial conditions. The system should be used at different soil water contents to obtain a full overview of the risk for overland flow from urban green areas.

#### 4.5 | Practical application

Runoff estimation from urban permeable surfaces is typically based on coupled infiltration and surface runoff models. The models are usually based on standard assumptions for different soils and surface types and are rarely subject to site-specific calibration, although experimental validation and calibration could substantially increase model quality. Furthermore, empirical data can help urban drainage engineers make the best decisions when choosing models to simulate urban green areas rainfall-runoff. Such decisions are important because urban green areas often constitute more than 50% of the total areas in the urban landscape. In this way, green areas could contribute to large quantities of runoff in periods where the infiltration capacity of the green surfaces are exceeded. The experiments presented in this study show that a good correlation can be found between soil water conditions and infiltration capacity, illustrating the potential for surface runoff. Moreover, the measurements seem to give a reliable estimate of the variation in infiltration and runoff distributed upon all possible soil water content levels. Therefore, these measurements could potentially be implemented as a site-specific infiltration term or used for site-specific infiltration model calibration. This approach will improve the quality of models, thereby improving the quality of urban drainage infrastructure.

The developed rainfall simulator could be a valuable tool to avoid severe overestimation or underestimation of runoff from urban permeable surfaces. Overestimation of urban green areas runoff in urban drainage models would result in larger dimensions of pipes, detention basins, and so forth. Therefore, this overestimation could increase the construction cost of the drainage network and is preferably avoided if possible. In contrast, underestimation of urban green area runoff would lead to smaller urban drainage dimensions, which could result in local inundation in urban areas, thereby increasing flood damage costs.

The ability of the rainfall simulator to produce variable historical rainfall events could be used to assess historical flood events and to determine the contribution of runoff from green areas during such rainfall events. Furthermore, as the soil water content seems to be well correlated with runoff, soil water content could be measured in real time in areas characterized by the rainfall simulator to continuously assess the potential of urban green surface runoff.

The measured relationships between infiltration, soil water content, and slope could potentially replace conventional models to estimate runoff urban drainage systems. Furthermore, relationships

between infiltration and slope could be implemented in geographic information system software for risk mapping of urban green areas that could potentially contribute significantly to the total runoff from urban surfaces. In this way, areas that should have increased attention can be identified.

## 5 | CONCLUSION

This study presents a method of constructing a novel rainfall simulator for the simulation of both constant and temporally variable rainfall events. A microcomputer controls the rainfall simulation, and the system can automatically reproduce rainfall events without manual intervention. The rainfall simulator is mobile and can be used to test the potential for surface runoff from pervious surfaces in multiple sites. The rainfall simulator has a good representation of natural rainfall and has a uniform spatial distribution of rainfall. Field tests show that the setup operates well under field conditions. However, wind can interfere with simulated raindrops. Therefore, it is recommended that the current setup be used under calm wind conditions or with wind shields.

This study applied the designed rainfall simulator to assess the runoff and infiltration characteristics of a grass-covered urban area. It was found that infiltration was strongly correlated with the soil VWC. The combination of steep slope and high soil water content resulted in the highest runoff rates and the lowest infiltration rates. Finally, the runoff coefficient depends on the soil VWC and cannot be constant under unsaturated conditions.

It was possible to derive a detailed and consistent relationship between runoff, infiltration, and soil water content conditions with the designed rainfall simulator. Therefore, the rainfall simulator could be useful in urban drainage design to derive runoff and infiltration relationships on the basis of soil water content. Such knowledge could be applied directly in surface runoff modelling or for calibration and validation of existing surface runoff models.

## FUNDING INFORMATION

This research was funded by the Foundation for Development of Technology in the Danish Water Sector, Innovation Fund Denmark, Aarhus Vand, EnviDan, and Aalborg University.



## ACKNOWLEDGMENTS

This research was funded by the Foundation for Development of Technology in the Danish Water Sector, Innovation Fund Denmark, Aarhus Vand, EnviDan, and Aalborg University.

## DATA AVAILABILITY STATEMENT

The data and scripts that support the findings of this study are available from the corresponding author upon reasonable request.

## ORCID

Kristoffer T. Nielsen  <https://orcid.org/0000-0001-8720-832X>  
Søren Thorndahl  <https://orcid.org/0000-0003-4654-6204>

## REFERENCES

- Abudi, I., Carmi, G., & Berliner, P. (2012). Rainfall simulator for field runoff studies. *Journal of Hydrology*, 454-455, 76-81. <https://doi.org/10.1016/j.jhydrol.2012.05.056>
- Adekalu, K. O., Olorunfemi, I. A., & Osunbitan, J. A. (2007). Grass mulching effect on infiltration, surface runoff and soil loss of three agricultural soils in Nigeria. *Bioresource Technology*, 98(4), 912-917. <https://doi.org/10.1016/j.biortech.2006.02.044>
- Arnaez, J., Lasanta, T., Ruiz-Flaño, P., & Ortigosa, L. (2007). Factors affecting runoff and erosion under simulated rainfall in Mediterranean vineyards. *Soil & Tillage Research*, 93(2), 324-334. <https://doi.org/10.1016/j.still.2006.05.013>
- Ashman, M., & Puri, G. (2013). *Essential soil science: A clear and concise introduction to soil science*. UK: John Wiley & Sons.
- Bartholomew, M. J. (2014). *Parsivel2 handbook (no. DOE/SC-ARM-TR-137)*. Upton, NY (United States): DOE Office of Science Atmospheric Radiation Measurement (ARM) Program (United States); Brookhaven National Laboratory (BNL).
- Benavides Solorio, J., & MacDonald, L. H. (2001). Post-fire runoff and erosion from simulated rainfall on small plots, Colorado front range. *Hydrological Processes*, 15(15), 2931-2952. <https://doi.org/10.1002/hyp.383>
- Burch, G., Moore, I., & Burns, J. (1989). Soil hydrophobic effects on infiltration and catchment runoff. *Hydrological Processes*, 3(3), 211-222. <https://doi.org/10.1002/hyp.3360030302>
- Campbell Scientific. (2010). ARG100 tipping bucket rain gauge Retrieved from <https://s.campbellsci.com/documents/eu/manuals/arg100.pdf>
- Campbell Scientific. (2014). CS451/CS456 submersible pressure transducer Retrieved from <https://s.campbellsci.com/documents/us/manuals/cs451-cs456.pdf>
- Campbell Scientific. (2018). CS650 and CS655 water content reflectometers Retrieved from <https://s.campbellsci.com/documents/us/manuals/cs650.pdf>
- Cerdà, A., Ibáñez, S., & Calvo, A. (1997). Design and operation of a small and portable rainfall simulator for rugged terrain. *Soil Technology*, 11(2), 163-170. [https://doi.org/10.1016/S0933-3630\(96\)00135-3](https://doi.org/10.1016/S0933-3630(96)00135-3)
- Christiansen, J. E. (1942). *Irrigation by sprinkling*. Berkeley, Cal: Agricultural Experiment Station Bull. 670.
- Clarke, M. A., & Walsh, R. P. D. (2007). A portable rainfall simulator for field assessment of splash and slopewash in remote locations. *Earth Surface Processes and Landforms*, 32(13), 2052-2069. <https://doi.org/10.1002/esp.1526>
- Dane, J. H., & Topp, G. C. (2002). *Methods of soil analysis: Part 4—Physical methods*. SSSA Book Series No. 5. Madison, USA: Soil Science Society of America.
- de Jonge, L. W., Jacobsen, O. H., & Moldrup, P. (1999). Soil water repellency: Effects of water content, temperature, and particle size. *Soil Science Society of America Journal*, 63(3), 437-442. <https://doi.org/10.2136/sssaj1999.03615995006300030003x>
- Gilley, J. E., & Finkner, S. C. (1985). Estimating soil detachment caused by raindrop impact. *Transactions of ASAE*, 28(1), 140-146. <https://doi.org/10.13031/2013.32217>
- Green, W. H., & Ampt, G. A. (1911). Studies on soil physics. *The Journal of Agricultural Science*, 4(1), 1-24. <https://doi.org/10.1017/S0021859600001441>
- Gregory, J. H. (2006). Effect of urban soil compaction on infiltration rate. *Journal of Soil and Water Conservation*, 61(3), 117-124.



- Groenendyk, D. G., Ferré, T. P. A., Thorp, K. R., & Rice, A. K. (2015). Hydrologic-process-based soil texture classifications for improved visualization of landscape function. *PLoS ONE*, *10*(6), e0131299. <https://doi.org/10.1371/journal.pone.0131299>
- Horton, R. E. (1939). Analysis of runoff-plot experiments with varying infiltration-capacity. *Eos, Transactions American Geophysical Union*, *20*(4), 693–711. <https://doi.org/10.1029/TR020i004p00693>
- Humphry, J. B. (2002). A portable rainfall simulator for plot-scale runoff studies. *Applied Engineering in Agriculture*, *18*(2), 199–204.
- Iserloh, T., Ries, J. B., Arnáez, J., Boix Fayos, C., Butzen, V., Cerdà, A., ... Wirtz, S. (2013). European small portable rainfall simulators: A comparison of rainfall characteristics. *Catena*, *110*, 100–112. <https://doi.org/10.1016/j.catena.2013.05.013>
- Keifer, C. J., & Chu, H. H. (1957). Synthetic storm pattern for drainage design. *ASCE Journal of the Hydraulics Division*, *83*(4), 1–25.
- Madsen, H., Gregersen, I. B., Rosbjerg, D., & Arnbjerg-Nielsen, K. (2017). Regional frequency analysis of short duration rainfall extremes using gridded daily rainfall data as co-variate. *Water Science and Technology*, *75*(8), 1971–1981. <https://doi.org/10.2166/wst.2017.089>
- Miller, W. P. (1987). A solenoid-operated, variable intensity rainfall simulator. *Soil Science Society of America Journal*, *51*(3), 832–834. <https://doi.org/10.2136/sssaj1987.03615995005100030048x>
- Nielsen, K. T., Moldrup, P., Thorndahl, S., Nielsen, J. E., Uggerby, M., & Rasmussen, M. R. (2019). Field-scale monitoring of urban green area rainfall-runoff processes. *Journal of Hydrologic Engineering*, *24*. [https://doi.org/10.1061/\(ASCE\)HE.1943-5584.0001795](https://doi.org/10.1061/(ASCE)HE.1943-5584.0001795)
- OTT Hydromet. (2011). *Operating instructions: Present weather sensor—OTT Parsivel<sup>2</sup>*.
- Paige, G. B. (2004). The walnut gulch rainfall simulator: A computer-controlled variable intensity rainfall simulator. *Applied Engineering in Agriculture*, *20*(1), 25–31. <https://doi.org/10.13031/2013.15691>
- Pan, C., & Shangguan, Z. (2006). Runoff hydraulic characteristics and sediment generation in sloped grassplots under simulated rainfall conditions. *Journal of Hydrology*, *331*(1-2), 178–185. <https://doi.org/10.1016/j.jhydrol.2006.05.011>
- Quinton, J. N., Edwards, G., & Morgan, R. (1997). The influence of vegetation species and plant properties on runoff and soil erosion: Results from a rainfall simulation study in south east Spain. *Soil Use and Management*, *13*(3), 143–148. <https://doi.org/10.1111/j.1475-2743.1997.tb00575.x>
- Redfern, T. W., MacDonald, N., Kjeldsen, T. R., Miller, J. D., & Reynard, N. (2016). Current understanding of hydrological processes on common urban surfaces. *Progress in Physical Geography*, *40*(5), 699–713. <https://doi.org/10.1177/0309133316652819>
- Sharma, K. D. (1986). Runoff behaviour of water harvesting micro-catchments. *Agricultural Water Management*, *11*(2), 137–144. [https://doi.org/10.1016/0378-3774\(86\)90026-0](https://doi.org/10.1016/0378-3774(86)90026-0)
- Sharpley, A. (2003). Effect of rainfall simulator and plot scale on overland flow and phosphorus transport. *Journal of Environmental Quality*, *32*(6), 2172–2179. <https://doi.org/10.2134/jeq2003.2172>
- Van Dijk, A. I. J. M., Bruijnzeel, L. A., & Rosewell, C. J. (2002). Rainfall intensity–kinetic energy relationships: A critical literature appraisal. *Journal of Hydrology*, *261*(1-4), 1–23. [https://doi.org/10.1016/S0022-1694\(02\)00020-3](https://doi.org/10.1016/S0022-1694(02)00020-3)

**How to cite this article:** Nielsen KT, Moldrup P, Thorndahl S, et al. Automated rainfall simulator for variable rainfall on urban green areas. *Hydrological Processes*. 2019;33:3364–3377. <https://doi.org/10.1002/hyp.13563>